Flywheels With All-Passive, Non-Contact Magnetic Suspensions

A.C. Day, M. Strasik, J. Mittleider, J. Edwards, P.E. Johnson, M.D. Higgins, J.R. Schindler, K.E. McCrary, R.A. Hawkins, D.L. Carlson[1]— A.E. Segall[2]

ABSTRACT

Flywheels are of interest for a wide range of energy storage applications, from support of renewable resources such as wind generation [1,2], to distributed power applications and uninterruptible power systems (UPS). The Boeing Company is designing and building prototype flywheels of 1 - 10 kWh total stored energy and has focused much of the effort on high-temperature superconducting (HTS) bearing systems. The use of such bearings has significant advantages for applications requiring large amounts of energy to be stored with low parasitic losses and with minimal system maintenance.

INTRODUCTION

Most flywheels now in development are suspended by ball bearings or active magnetic bearings. Permanent magnets may also be used to support much of the weight of the flywheel and reduce the thrust load on the primary bearings. For ball bearings the life and vacuum compatibility are serious issues and the rotor must be extremely well balanced. Control speed and reliability are common problems for active magnetic bearings. Shaft heating is a concern for either approach. The flywheels now offered for sale are able to produce significant amounts of power (to hundreds of kW) but store at most only a few kWh of energy. For applications such as peak shaving, load leveling, and many data centers, much more energy must be stored. This will necessitate larger flywheels. A simple doubling of all dimensions will result in eight times the mass and energy but only increase the shaft areas by a factor of four. Thus, the already-challenging issues of high contact stresses and limited heat transfer will become significantly more difficult for the established bearing technologies. Superconducting bearings offer a potential way to overcome these difficulties and gain an order of magnitude or more in flywheel storage capacity.

Superconducting suspension using the Meissner effect and flux pinning has been known for many decades. The most common arrangement requires one or more rings of permanent magnet in the rotor, which are in proximity to a number of superconductor bulks in the stator [3]. The magnetic fields produced by the rings penetrate the superconductors prior to chilling. After chilling of the HTS, the field pattern becomes effectively "pinned" in the superconductors since very high surface currents (approaching 10^5 A/cm^2) will spontaneously oppose changes in the local flux density. Practical bearings based on this phenomenon have become economically feasible only in the last several years due to the discovery and development of the high-temperature superconducting compounds, including $YBa_2Cu_3O_{7-x}$ (YBCO) [4]. Flywheels of at least 300lb. have been spun to high speeds on HTS bearings and systems with capacities to 10 MWh are being seriously considered [5].

HTS BEARING CHARACTERISTICS

We have been working to develop HTS bearing technology that will be scaleable from small (a few kWh) to mid-size (several tens of kWh) or larger flywheels [6]. Over the past two years we have built and tested a bearing that is based on a nominal 10 kWh flywheel design for operation at 20,000 rpm. The bearing has been tested by itself and with a 100 lb. / 1 kWh rotor.

A photo of the magnet assembly on a small test rotor (20 lb. total weight) is shown in figure 1. It consists of several rings of radially-polarized magnets, together with steel pole rings that turn the flux outward and through the superconductors. The assembly is normally oriented facedown and positioned several mm above a LN-

[1] Boeing Phantom Works, Seattle WA. Email: arthur.c.day@boeing.com
This work is supported in part by the U.S. Department of Energy's Office of Power Technology through the Superconductivity Program and the Energy Storage Program.
[2] Washington State University, Vancouver, WA.

cooled cryostat containing YBCO crystals. The bearing stiffness was optimized by using finite-element modeling to maximize the field gradients within the crystals. The crystal array for this bearing is affixed to the underside of the cryostat lid as shown in figure 2. We are able to cool the crystals with gravity-fed nitrogen at 77 K or with a closed-loop refrigeration system at temperatures to 65 K.

Figure 1. Magnet assembly for an HTS bearing, shown here installed on a bearing test rotor. This assembly is suitable for flywheels of up to several hundred pounds.

To date, the test rotor has been spun up to 15,000 rpm using an eddy current clutch. The time history of a typical test run, shown in figure 3, exhibits several acceleration and deceleration ramps and also a number of free coasting periods. By mechanically decoupling the clutch system we can accurately measure bearing losses through the coasting spin-down rates. The loss power P is given by

$$P = R \times J \times S \times 4\pi^2/60^3$$

where R is the spin-down rate in rpm/minute, J is the polar moment of inertia in kg-m^2, and S is the speed in rpm. Figure 4 shows spin-down rates measured at speeds to 15,000 rpm and extrapolated to the design speed of 20,000 rpm. Various data sets show effects of speed and temperature, discussed below; also, that the bearing performance has improved over the past year as we made basic provisions for balance and alignment.

There are two major contributors to the spin-down rate: the so-called AC loss that is dissipated in the superconductors, and eddy current losses due to motion of the not-quite-symmetric magnets near metallic conductors [7]. The AC loss normally shows little if any speed dependence, i.e., the loss per revolution is nearly constant. The eddy current loss is speed dependent and goes to zero at low speeds. Referring to figure 4, the AC loss is thus inferred from the Y-intercept while the balance of the loss is due mainly to eddy currents. Variation of the test chamber pressure showed that windage losses were minimal. The increase in spin-down rate from 300 – 1000 rpm is due to vibration near the bearing resonance but is not important for determining normal operating losses.

Figure 2. YBCO crystal array on underside of cryostat lid. Displacement of rotor magnets leads to large response currents in superconductors, passively restoring rotor position at any speed.

It is important to note that only the AC loss must be removed by the refrigeration system. Eddy current losses are usually subject to reduction by several means and in any case amounted to only a few watts in these tests. The callouts in figure 4 show the net effect of applying an appropriate refrigeration penalty of 20X to the AC loss components and adding these to the existing eddy current contributions. Figure 4 also shows the effect of changing the cryogen temperature by six degrees. The current density J_c in YBCO typically increases by a factor of about 1.5 between 77 K and 71 K, while superconductor loss models predict an inverse-cube dependence on J_c. The Y-intercept drops by about a factor of two between these temperatures. The net cooling power required for the bearing could then be as little as 6.8 W at 20,000 rpm, again without assuming any reduction in the eddy current contribution.

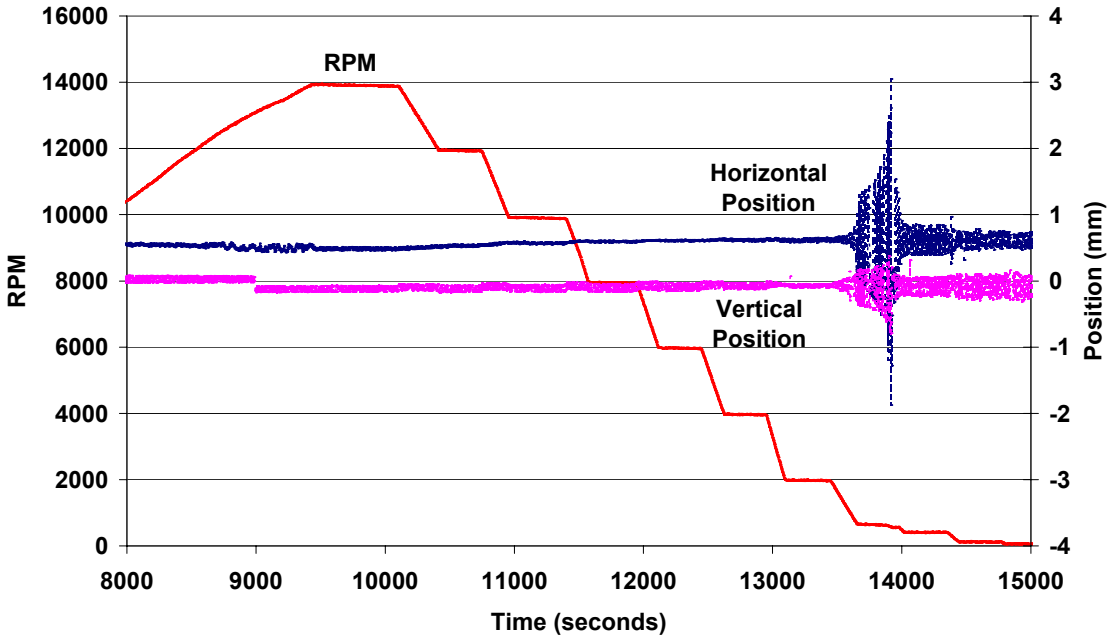

Figure 3. Typical HTS bearing test run, showing a number of coasting periods for measurement of losses. Rotor position envelopes indicate vibration amplitude and show bearing critical speed at 700 rpm.

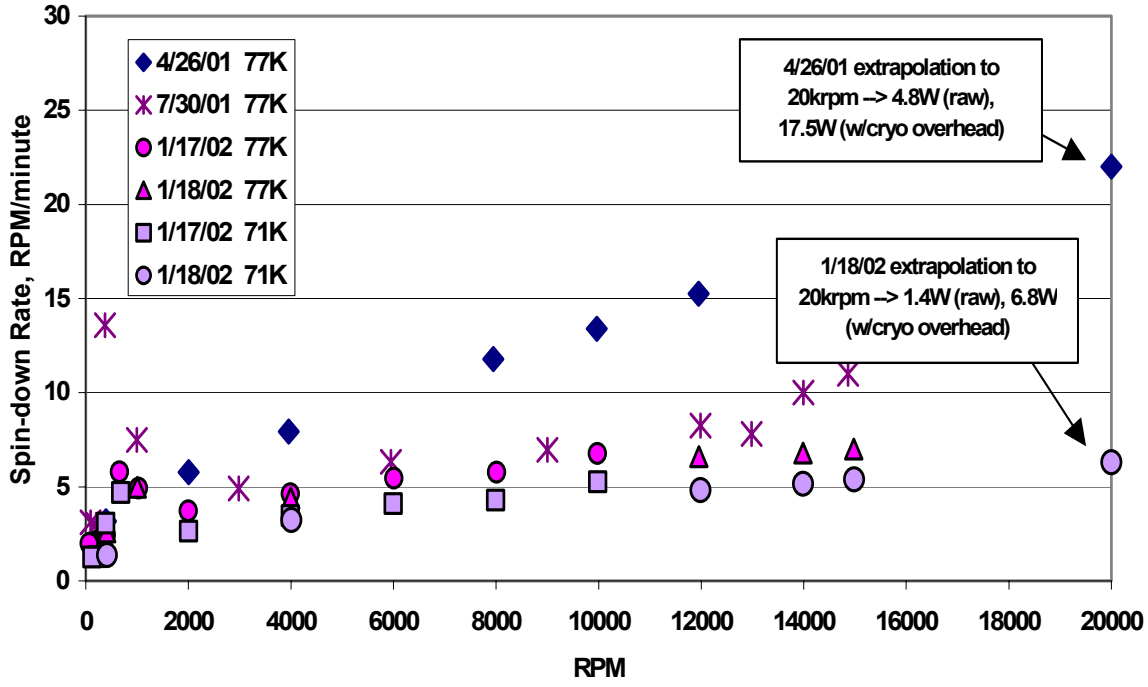

Figure 4. Bearing spin-down rate data showing speed dependence, YBCO temperature effects, and trend of improvements over past year. Analysis of speed dependence was used to separate cryogenic and non-cryogenic power sinks and to extrapolate to net performance at 20,000 rpm.

The bearing is very simple dynamically. Figure 3 showed the envelope of horizontal motion of the test rotor through a 14,000-rpm run. Apart from the rigid-body resonance at approximately 700 rpm the traces show only surface runout – i.e., no vibrational modes. This fact underscores the simplicity and robustness of the passive HTS bearing when compared with the sensors, actuators, control algorithms, and tuning needed for active-bearing systems.

DEMONSTRATION OF FLYWHEELS WITH HTS BEARINGS

A relatively simple and low-cost rotor was constructed to demonstrate the ability of an HTS bearing to suspend and spin a significant mass, in this case 100 lb. including the magnets and hub. The basic construction of this rotor is shown in figure 5. The splined hub design was due originally to Toray Composites and was modified by Boeing to reduce mass.

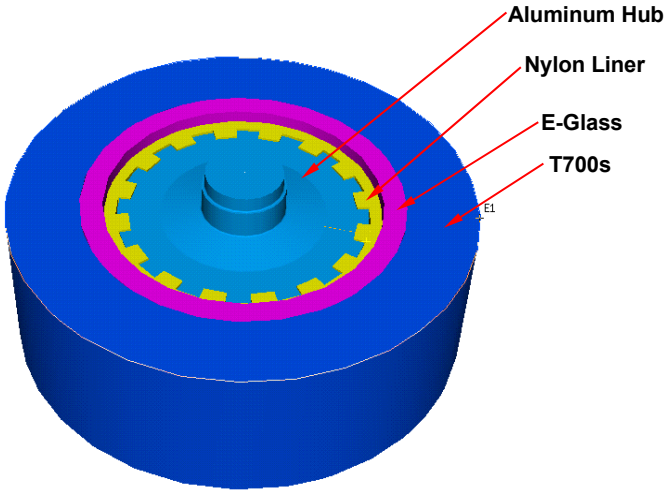

Figure 5. 1 kWh rotor with Toray/Boeing G-S hub design.

Early in 2001, an eddy-current clutch was used to spin the rotor to speeds up to 8,000 rpm. Only relatively minor problems with a new cryogenic system prevented us from taking the rotor to higher speeds at that time. In February of 2002 modifications were made to this rotor to adapt a 3 kW motor/generator to the shaft. The complete flywheel is shown in figure 6. The motor/generator and a lift magnet ring are above the rim while the main magnet assembly is located below. At the rim's rated speed of 24,000 rpm this wheel would yield a stored energy of approximately 1 kWh while maintaining a factor of safety of 2. Spin-testing of this flywheel began in March and showed the basic ability to levitate and handle motor torque at low speeds, including through the bearing critical. Motor control problems have slowed progress somewhat but we hope to achieve speeds above 10,000 rpm soon.

In a parallel effort we have been designing and testing components for a 10 kWh / 20,000 rpm flywheel. The main structure of the wheel is shown in figure 7 after spin testing on a quill. The bearing, motor, and lifting magnets have been tested separately and are now being added to the flywheel hub. Levitation and spinning of the full flywheel are planned for April and May of 2002.

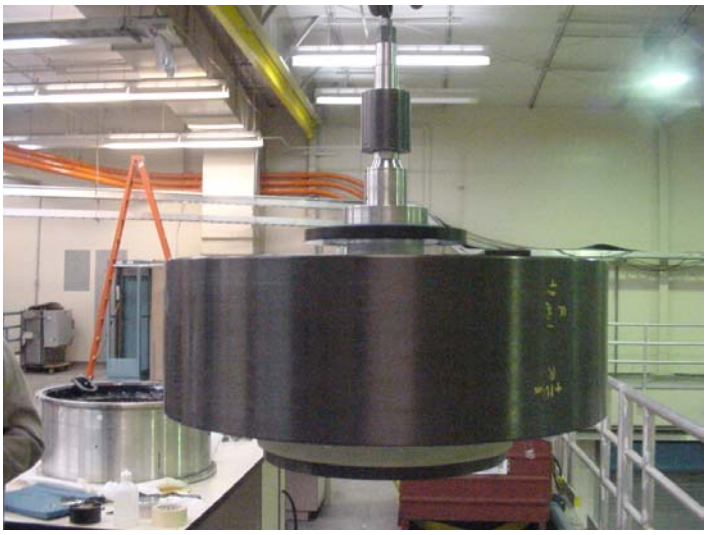

Figure 6. Completed 1 kWh flywheel. Lift magnet and motor rotor are above the rim; magnet assembly for HTS bearing is below.

Figure 7. Rotor for a 10 kWh flywheel after quill test at 14,000 rpm. Rotor is being integrated with an HTS bearing and a motor/generator for a lab demonstration of flywheel stability.

MAGNET MATERIAL CONSIDERATIONS

The ability of the magnets to withstand rotation-induced stresses is a key design consideration. For metals and other ductile materials, vendor-supplied strength data are often adequate for design. Because magnets are brittle materials whose failure is chiefly due to tiny flaws, it is more appropriate to use a statistical approach (i.e., Weibull parameters) to characterize their strength and reliability. Vendor data seldom contain this level of detail so we began a focused study to characterize a good grade of magnet material, a NdFeB rare-earth magnet with an energy product of approximately 43 MGOe.

The fracture strength and related statistical measures are dependent on the size and surface of the fracture specimens. All surface preparations and the resulting finish of the fracture specimen must be kept as close as possible to the components' as-used state. In order to meet these mandates, a 4-point bend test protocol known as Modulus of Rupture (MOR) was adopted for the current study. This in turn required that the vendor fabricate the rectangular "bend" specimens by using their standard shaping and grinding operations. In addition, three samples were also shaped using a wire EDM in order to evaluate the ramifications of using this process. A total of twenty-five 0.197in x 0.197in x 1.97in rectangular samples were supplied for testing. All MOR fracture tests were conducted in accordance with ASTM Standard C1161 except that the surface finish was in the ground condition characteristic of their standard manufacturing process. The distribution of fracture stresses is shown in figure 8; the reduced data in terms of Weibull parameters are given in Table 1.

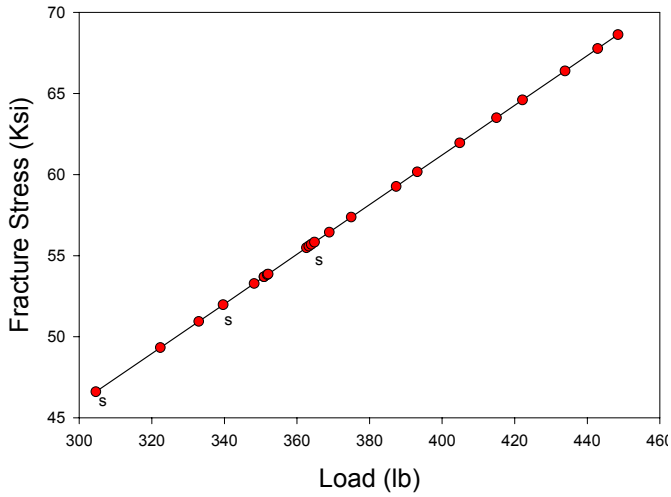

Figure 8. Failure loads and stresses for NdFeB magnet specimens. Samples with EDM surface are shown with "s".

Material	Modulus m	σ_{ave} (Ksi)	σ_{oA} (Ksi-in$^{2/m}$)	σ_{oA} (Ksi-in$^{3/m}$)
NdFeB magnet: energy product = 43 MGO	9.6	57.2	98.5	84.0

Table 1. Unit Weibull parameters and average fracture strength data measured for NdFeB magnet samples. σ_{ave} is the average strength, σ_{oA} and σ_{oA} are the characteristic strengths for area and volume, respectively.

If the stress field through a part can be measured or calculated, the Weibull parameters can be used to generate the failure probability due to each small volume, and ultimately for the entire part. It is assumed that the flaws are distributed randomly in both the parts and in the original test specimens. The final step in our magnet material study was to calculate the stress fields throughout the magnet assembly at a series of speeds and apply the above parameters to arrive at a net probability of failure. The result was a failure probability of 10^{-6} for the magnets at a speed of 26,000 rpm, well above our design speeds for both the 1 kWh and 10 kWh flywheels.

CONCLUDING REMARKS

This paper has discussed the attributes of HTS bearings and given examples of test performance of our 10 kWh bearing design. Our current design approach, to use one or more rings of horizontally-polarized permanent magnet with steel poles, is scaleable from a rotors of a few pounds to flywheels of at least the 50 kWh class. Related approaches are being considered for flywheels up to the MWh class. An overview of bearing assemblies either designed and/or tested at Boeing is shown in Table 2 below. In our assessment of flywheel systems, the benefits of the HTS bearings will become compelling for systems of tens of kWh of storage even when the cryogenic subsystem is included. In addition to potential efficiencies of operation these bearings have been shown to be simple to operate and are tolerant of relatively large rotor unbalances.

Test Article	Weight (approx.)	# Magnet Rings	Diameter	Speed (rpm)
Bearing (1996)	**5 lb.**	**1**	**6”**	**5,000 tested**
Bearing (2000-2002)	**20 lb.**	**3**	**9”**	**15,000 tested 24,000 design**
1 kWh Flywheel (2001-2002)	**100 lb.**	**3**	**9”**	**8,000 tested 24,000 design**
10 kWh Flywheel (2002-2003)	**400 lb.**	**3**	**9”**	**12-15,000 tested 20,000 design**
50 kWh Flywheel (future)	**1500-2000 lb.**	**4**	**12” (approx.)**	**12-16,000 design**

Table 2. Scaling of HTS bearing designs using planar magnet approach.

REFERENCES

1. Infield, D.G., “Wind/Diesel System with Flywheel Energy Storage,” IEA Workshop on Wind-Diesel Systems, Rutherford Laboratory, England, June 1987.
2. Genta, G., “Kinetic Energy Storage”, Butterworths, Boston (1985).
3. Hull, J., Hilton, E., Mulcahy, T., Yang, Z., Lockwood, A., and Strasik, M., J.Appl. Phys. **79** (1996).
4. Hicks, W.C., Dogan, F., Strasik, M., Day, A.C., and McCrary, K.E., “The Effect of Platinum and Excess 211 Phase on the Loss of the Liquid Phase in Melt Textured $YBa_2Cu_3O_{7-x}$”, IEEE Transactions on Applied Superconductivity **9** (2), pp. 2060-2065 (1999).
5. Project by Japan’s NEDO consortium.
6. Day. A.C., Strasik, M., Wood, J., Taylor, P., and Johnson, L.C. “Development of Long-life, Low-maintenance Flywheel Electricity Systems”, Presented in proceedings of EESAT 2000, Sept. 18-20 2000, Orlando, FL.
7. Hull, J.R., and Cansiz, A., “Vertical and Lateral Forces Between a Permanent Magnet and a High-Temperature Superconductor”, J. Appl. Phys. **86** (11), 6396 (1999).

Material	Modulus m	σ_{ave} (Ksi)	σ_{oA} (Ksi-in$^{2/m}$)	σ_{oA} (Ksi-in$^{3/m}$)
NdFeB magnet: energy product = 43 MGO	9.6	57.2	98.5	84.0

Table 1. Unit Weibull parameters and average fracture strength data measured for NdFeB magnet samples. σ_{ave} is the average strength, σ_{oA} and σ_{oA} are the characteristic strengths for area and volume, respectively.

If the stress field through a part can be measured or calculated, the Weibull parameters can be used to generate the failure probability due to each small volume, and ultimately for the entire part. It is assumed that the flaws are distributed randomly in both the parts and in the original test specimens. The final step in our magnet material study was to calculate the stress fields throughout the magnet assembly at a series of speeds and apply the above parameters to arrive at a net probability of failure. The result was a failure probability of 10^{-6} for the magnets at a speed of 26,000 rpm, well above our design speeds for both the 1 kWh and 10 kWh flywheels.

CONCLUDING REMARKS

This paper has discussed the attributes of HTS bearings and given examples of test performance of our 10 kWh bearing design. Our current design approach, to use one or more rings of horizontally-polarized permanent magnet with steel poles, is scaleable from a rotors of a few pounds to flywheels of at least the 50 kWh class. Related approaches are being considered for flywheels up to the MWh class. An overview of bearing assemblies either designed and/or tested at Boeing is shown in Table 2 below. In our assessment of flywheel systems, the benefits of the HTS bearings will become compelling for systems of tens of kWh of storage even when the cryogenic subsystem is included. In addition to potential efficiencies of operation these bearings have been shown to be simple to operate and are tolerant of relatively large rotor unbalances.

Test Article	Weight (approx.)	# Magnet Rings	Diameter	Speed (rpm)
Bearing (1996)	**5 lb.**	**1**	**6”**	**5,000 tested**
Bearing (2000-2002)	**20 lb.**	**3**	**9”**	**15,000 tested 24,000 design**
1 kWh Flywheel (2001-2002)	**100 lb.**	**3**	**9”**	**8,000 tested 24,000 design**
10 kWh Flywheel (2002-2003)	**400 lb.**	**3**	**9”**	**12-15,000 tested 20,000 design**
50 kWh Flywheel (future)	**1500-2000 lb.**	**4**	**12” (approx.)**	**12-16,000 design**

Table 2. Scaling of HTS bearing designs using planar magnet approach.

REFERENCES

1. Infield, D.G., “Wind/Diesel System with Flywheel Energy Storage,” IEA Workshop on Wind-Diesel Systems, Rutherford Laboratory, England, June 1987.
2. Genta, G., “Kinetic Energy Storage”, Butterworths, Boston (1985).
3. Hull, J., Hilton, E., Mulcahy, T., Yang, Z., Lockwood, A., and Strasik, M., J.Appl. Phys. **79** (1996).
4. Hicks, W.C., Dogan, F., Strasik, M., Day, A.C., and McCrary, K.E., “The Effect of Platinum and Excess 211 Phase on the Loss of the Liquid Phase in Melt Textured $YBa_2Cu_3O_{7-x}$”, IEEE Transactions on Applied Superconductivity **9** (2), pp. 2060-2065 (1999).
5. Project by Japan’s NEDO consortium.
6. Day. A.C., Strasik, M., Wood, J., Taylor, P., and Johnson, L.C. “Development of Long-life, Low-maintenance Flywheel Electricity Systems”, Presented in proceedings of EESAT 2000, Sept. 18-20 2000, Orlando, FL.
7. Hull, J.R., and Cansiz, A., “Vertical and Lateral Forces Between a Permanent Magnet and a High-Temperature Superconductor”, J. Appl. Phys. **86** (11), 6396 (1999).